

New exploration of bladder cancer-related immune gene biomarkers in predicting the prognosis of urinary system tumors

Jun Zheng (✉ 2020120934@stu.cqmu.edu.cn)

Kuanren Hospital: The Second Affiliated Hospital of Chongqing Medical University

<https://orcid.org/0000-0002-8141-5413>

Junyong Zhang

Kuanren Hospital: The Second Affiliated Hospital of Chongqing Medical University

Weili Zhang

Kuanren Hospital: The Second Affiliated Hospital of Chongqing Medical University

Research

Keywords: Immune-related genes, Prognosis, Bladder cancer, Clear cell renal cell carcinoma

Posted Date: January 31st, 2022

DOI: <https://doi.org/10.21203/rs.3.rs-1238760/v1>

License:   This work is licensed under a Creative Commons Attribution 4.0 International License.

[Read Full License](#)

Abstract

Background: Bladder cancer (BLCA) ranks first among genitourinary system tumors in terms of its incidence, and it is associated with poor prognosis due to its high recurrence and metastasis rates. In recent years, in-depth research on tumor microenvironment (TME) and immune infiltration has greatly improved the management of urinary system tumors, especially for advanced BLCA. Therefore, this study aimed to construct a risk scoring model with related immune genes as the independent prognostic factors, so as to estimate BLCA survival according to immune gene expression characteristics.

Methods: Here, we downloaded clinical and mRNA data of BLCA in TCGA database and utilized them as the model test set. Clinical samples with incomplete tumor staging or grading information were excluded from this study. Differentially expressed genes (DEGs) between BLCA and normal tissues were identified for GO and KEGG functional enrichment. Further, the prognostic DEGs were obtained by screening the identified DEGs. Thereafter, univariate, multivariate and Lasso regression analyses were performed on immune genes from the as-identified prognostic DEGs. As a result, four independent related immune genes (OAS1, APOBEC3H, LBP1, ANHAK) were obtained, which were then incorporated in the construction of an immune risk scoring model. Finally, TCGA-clear cell renal cell carcinoma (CCRCC) was used as a validation set to validate the risk model.

Results: Upon multivariate analyses of both test and validation sets, the four independent genes used to construct the risk scoring model were the independent prognostic factors. As revealed by Kaplan-Meier (KM) curve of BLCA, patient survival time showed significant negative relation to risk score, as verified in validation set. Moreover, the receiver operating characteristic (ROC) curve suggested that, the area under the curve (AUC) was greatly improved when the risk score was used in combination with clinical characteristics, revealing that the risk score might have a better diagnostic value in clinic.

Conclusion: This study builds an immune risk assessment model based on the relationship between immunity and BLCA. Finally, four immune-associated prognostic genes were obtained, and the applicability of the model constructed using these four genes to predict urinary system tumors was verified.

1. Introduction

Nearly 200,000 people die of bladder cancer (BLCA) every year worldwide, and this number is constantly increasing (Siegel, Miller, & Jemal, 2015). Hematuria is the early stage of BLCA, which is often missed because it is covered by other urological diseases such as urinary tract stones and urinary tract infections. Transurethral resection of bladder tumor is the main treatment for non-invasive BLCA (Sanjeev Sharma, 2009). The necessity of combined bladder perfusion and second surgical resection is determined according to the size and scope of the tumor. However, BLCA still maintains high recurrence and metastasis rates after operation. Although radical cystectomy is the standard treatment for muscle-invasive BLCA, it still has high complication and mortality rates (Degeorge, Holt, & Hodges, 2017;

Hendricksen & Witjes, 2007). In this case, more and more emphasis has been placed on alternative treatments.

As we all know, BLCA is an inflammation-related disease. Chronic inflammation has been confirmed to be related to the progression of BLCA(Mbeutcha et al., 2016; Yang, Chang, Meng, Gao, & Wang, 2018). On the one hand, during tumor development, inflammatory factors can initiate cell repair and regeneration by stimulating immune system responses(Karin & Clevers, 2016; Wallach et al., 2014). On the other hand, inflammation can also be triggered by genotoxic and oxidative stresses resulting from carcinogens, smoking and drinking.(Candido & Hagemann, 2013; Mantovani, Allavena, Sica, & Balkwill, 2008)

Tumor microenvironment (TME) has immunoregulatory properties, and the immune system can generate anti-tumor immunity by affecting tumor growth and mutation behaviors. At the same time, tumor cells can damage immune cells in different ways(Fridman, Zitvogel, Sautes-Fridman, & Kroemer, 2017; Gandellini et al., 2015). Immunotherapy has gradually become an increasingly attractive strategy and has been clinically applied and verified(Jia et al., 2017; Spigel et al., 2018; Thomas et al., 2014; Vari et al., 2018). However, similar to other treatments, immunotherapy is only effective on a small number of urinary system tumors(Hoos et al., 2010; Mathieu et al., 2018; Peinemann, Unverzagt, Hadjinicolaou, & Moldenhauer, 2019). Therefore, one or more biomarkers are needed to identify patients most likely to respond to cancer and to determine their prognosis. The present work downloaded mRNA and complete clinical data of BLCA patients from TCGA database, and explored the association of immune mechanisms with BLCA. In summary, this study suggests that immune-related genes have important function effects and identifies the possible prognostic markers for BLCA for predicting urinary system tumor survival.

2. Materials And Methods

2.1 Material collection and data analysis tools

The data sets of BLCA and clear cell renal cell carcinoma (CCRCC) were obtained from TCGA database, including transcriptome data, complete clinical and survival information. The BLCA data set with complete information, including 19 normal samples and 414 tumor sample, was used as the test set. A total of 533 clinical samples of CCRCC were collected as the validation set. Samples with incomplete survival information or those with survival time less than 40 days were removed from the validation set, since these samples made it impossible to determine the correlation between the cause of patient death and the tumor.

Altogether 2483 immune genes were downloaded in immunology database and the analysis portal (ImmPort) database.

2.2 Differential expression analysis

According to gene levels within BLCA, firstly, we conducted differential gene analysis to determine differentially expressed genes (DEGs) between cancer and healthy tissues. Thereafter, the non-parametric methods were utilized to screen genes related to prognosis. In this study, DEGs were obtained by the DESeq2 package in R software, whereas prognostic genes were acquired through the survminer package and survival package in R software. The gene screening criteria were shown below, $\text{Log}_2|\text{FC}| > 1$ and $\text{padj} < 0.01$. In addition, the ggplot2 package in R software was used for statistical analysis and visualization of volcano plots.

2.3 Gene enrichment analysis

Gene Oncology (GO) functional annotation was conducted to evaluate the molecular functions (MFs), biological processes (BPs) and cellular components (CCs) of genes. Furthermore, Kyoto Encyclopedia of Genes and Genomes (KEGG) was adopted to integrate genomic, chemical and system function information and to perform pathway enrichment. The limit was set to $P < 0.05$, the org.Hs.eg.db package in R software was used for ID conversion, the clusterProfiler package was adopted in enrichment analysis, and the ggplot2 package was utilized for visualization.

2.4 Characteristics of immune genes-based risk score

The 1422 immune genes co-expressed by BLCA and DEGs were analyzed by intersection analysis to obtain the differential immune genes, which were later crossed with prognostic genes to acquire the prognostic differential immune genes. Afterwards, this study performed multivariate Cox regression for obtaining regression coefficients of independent prognostic factors. Immune Risk Scoring Characteristics (IRSS) was determined according to multiple Cox regression. Its formula was shown below, $h(t) = h_0(t) \exp(\beta_1 x_1 + \beta_2 x_2 + \dots + \beta_j x_j)$, where $h(t)$ is the risk function of the research object, which changes with time; x_1, x_2, \dots, x_j stand for independent variables, while $\beta_1, \beta_2, \dots, \beta_j$ are the regression coefficients (Zeng et al., 2017). After obtaining the risk score for every TCGA-BCLA sample, all cases were classified as high- and low-risk groups based on the median risk score. Next, we used Kaplan-Meier (KM) curve analysis for comparing overall survival (OS) of both groups. The area under receiver operating characteristic (ROC) curve (AUC) was calculated for analyzing prognostic value of IRSS for BLCA patients (DeLong, DeLong, & Clarke-Pearson, 1988).

2.5 Combination of risk score with clinical information and model validation

Univariate Cox regression was carried out for analyzing the association of IRSS with OS, meanwhile, we conducted multivariate Cox regression to assess the feasibility of IRSS as the independent predictor. The nomogram was obtained by integrating different clinical information, including age, gender, risk score and stage, so as to evaluate patient survival. Besides, decision curve analysis (DCA) was used for

evaluating the suitability of our as-constructed nomogram in clinical applications. In addition, TCGA-CCRCC was adopted to further verify the applicability of the as-established model in urinary system tumors.

3. Results

3.1 Differential analysis

First, we collected 395 samples with complete prognostic and gene expression profiles as an experimental group. To identify DEGs predicting BLCA patient survival, DEGs and clinical prognosis-related genes were screened between the tumor group and the normal group. As a result, 6588 DEGs and 527 prognostic genes were identified. Thereafter, the volcano map was plotted to visualize the DEGs(Figure1A). Furthermore, DEGs and immune-related genes were intersected to obtain 371 differential immune genes(Figure1B), which were later intersected with prognostic genes to yield 8 final prognostic differential immune genes(Figure1C). Parameter selection was completed by using the LASSO model through ten-fold cross-validation(Figure1D).

3.2 Development of a TCGA immune gene prognostic model

First, correlation of eight immune-related differential genes was displayed by the chord diagram(Figure2A). As revealed by univariate analysis, five of the seven genes were positively related genes (PTGER3, OGN, GHR, LRP1, AHANK), whereas the rest two were negatively related ones (OAS1, APOBEC3H) (Figure2B). Upon multivariate analysis, only four genes were included in model construction, including two negatively related genes (OAS1, APOBEC3H) and two positively related ones (LRP1, AHANK) (Figure2C). Furthermore, based on risk scores of the four prognostic differential immune genes, a risk distribution map and a risk score gene heat map were obtained(Figure2D 2E). Altogether 395 patients were equally classified as high-risk or low-risk subgroup. As revealed by K-M curve, OS was significantly different between both groups(Figure2G)($p < 0.001$).

3.3 Predictive evaluation of the risk model

Next, univariate and multivariate analyses were conducted for evaluating whether risk score served as the independent predictor. As a result, the risk score showed a strong correlation in both univariate (HR = 1.893, 95% CI:1.620-2.212, $P < 0.01$)(Figure3A) and multivariate analyses (HR = 1.722, 95% CI:1.454-2.039, $P < 0.01$) (Figure3B). The AUC was greatly improved when combining risk score and clinical information(Figure3C). Thereafter, the nomogram was obtained by integrating the risk score and clinical information(Figure3D). Besides, calibration curve revealed that survival prognosis predicted by the model well matched the actual patient prognosis(Figure3E).

3.4 Gene enrichment

First of all, as suggested by results of gene enrichment analysis of all differentially expressed genes, the genes were mainly enriched in muscle synthesis and processing(Figure4A 4B). With 50 genes as the limit, we conducted GO and KEGG analyses to explore main functions and pathways enriched by the up-regulated and down-regulated DEGs in BLCA cohort. As a result, DEGs were mainly enriched in multiple BPs, among which, up-regulated DEGs were mainly related to antibacterial humoral response and protein enzyme activity(Figure4C), whereas down-regulated DEGs were associated with protein assembly(Figure4D).

3.5 Validation of the external risk models

Data from 530 CCRCC cases of TCGA cohort were used as validation set. Based on median risk score, CCRCC cases were classified as high-risk (n=265) or low-risk (n=265) group, with significant difference in OS ($P < 0.001$)(Figure5A). As shown by the risk status chart, the patients were well divided into two groups, and the dead patients were concentrated in the high risk score area(Figure5C 5D). Both univariate and multivariate analyses were conducted to assess whether risk score independently predicted CCRCC. Finally, risk score was identified to independently predict prognosis upon univariate and multivariate Cox regression(Figure5E 5F).

3.6 Correlation between model genes and clinicopathological parameters

Both univariate and multivariate validated that risk score independently predicted prognosis of urinary system tumors. Therefore, we further explored the clinical relevance of four genes in BCLA. As a result, OAS1, AHNAK and LRP1 showed significant differences in tumor T staging, while only ANHAK exhibited significant significance between smoker and non-smoker groups. Further, there were significant differences in tumor N staging and STAGE staging among the four genes(Figure6 7 8 9). This prognostic model may be more suitable for staging as a reference and more meaningful in higher clinical stages.

3.7 Immune cell infiltration analysis

The infiltration of six immune cells in BCLA for the four genes was obtained using TIMER. The results showed that ANHAK and the six immune cells were significantly different, while neutrophils were significantly related to the four genes. In addition, the immune infiltration patterns of the four genes were not the same. To be specific, LRP1 was significantly positively related to CD8+T CELL macrophages, CD4 cells, neutrophils and dendritic cells (DCs). The different gene immune infiltration patterns in tumors indicate that immune infiltration may be involved in the construction of prognostic models, and the immune infiltration characteristics of genes may be related to the accuracy of the model.

4. Discussion

Immunotherapy of BLCA has attracted increasing attention. On the other hand, neoadjuvant therapy has a certain effect on reducing tumor staging to prevent cystectomy (Rey-Cárdenas, Guerrero-Ramos, Lista, Carretero-González, & Velasco, 2021; Yu, Ballas, Skinner, Dorff, & Quinn, 2017). However, research on immune-related markers for BLCA has not well established the clinical prognosis of tumors. Here, we selected BLCA differential genes and prognostic genes upon the threshold of $P < 0.01$. On this basis, four immune-related differential genes were obtained and an immune prognostic model of BLCA was established. Thereafter, TCGA-CCRCC was used as the validation set, and the feasibility of this model in immune-related prognostic model for urinary system tumors was finally determined.

As a member of the OAS family of interferon-induced antiviral enzymes, OAS1 is also an ancient immune-related gene (Hornung, Hartmann, Blässer, & Hopfner, 2014). But its prognostic value is rarely studied at present. Previous studies have shown that the high expression of OAS 1 in cancer cells promotes cell viability by mediating the DNA damage mechanism (Kondratova, Cheon, Dong, Holvey, & Stark, 2020; Padariya et al., 2021). OAS1 is most closely related to neutrophil infiltration in breast cancer (BC), and its high expression predicts poor prognosis of tumor (Zhang & Yu, 2020). As reported by the latest research, OAS1 is involved in the apoptotic process of microRNA-145 in human BLCA cells (Noguchi et al., 2013). This study illustrated the value of OSA1 as an immune-related gene, and its pathogenic mechanism should be further investigated.

As for the APOBEC3 enzyme family, the intrinsic immune defense against viruses is the endogenous source of somatic mutations in numerous human cancers (Constantin, Dubuis, Conde-Rubio, & Widmann, 2021). APOBEC3H (A3H) is the most polymorphic in human APOBEC3 genes, and APOBEC mutation represents the main mutation mode of TCGA-BLCA (Alexandrov et al., 2013; Gu et al., 2016). It has been previously reported that the mutation of APOBEC significantly improves the survival rate of TCGA-BLCA patients as a tumor suppressor gene, and APOBEC-mediated mutations are the possible reasons for the overexpression of FGFR3 mutations in BLCA (Shi et al., 2019). In head and neck cell carcinoma, high APOBEC3H level has an important effect on the immune infiltration and activation of CD8+ T cells (Q. Liu, Luo, Cao, Pan, & Ren, 2020). Therefore, it is reasonable to speculate that the infiltration of A3H in neutrophils may be involved in somatic mutations and affect patient survival.

In the LDLR family, LRP-1 represents the multifunctional scavenger receptor that not only controls different protease and growth factor levels, but also supports the morphology and function of tumor blood vessels (Dedieu & Langlois, 2008; Lillis, Duyn, Murphy-Ullrich, & Strickland, 2008; Theret, Jeanne, Langlois, Hachet, & Dedieu, 2017). It seems to play a decisive role in tumor progression. As a key regulator of the Notch pathway, LRP1 mediates cell growth and differentiation (Grigorenko, Moliaka, Soto, Mello, & Rogaev, 2004). In esophageal squamous cell carcinoma (ESCC), LRP1 affects patient prognosis by inducing the migration and invasion of tumor cells and macrophages (Sakamoto, Koma, Higashino, Kodama, & Yokozaki, 2021). Besides, LRP1 has the strongest correlation with macrophage infiltration in

BCLA. It is speculated that macrophages may increase the carcinogenicity of tumor cells through immune infiltration in tumor cells.

AHNAK2 is a key protein for cell migration. Its deletion leads to an increase in p53 reactivity, which affects cancer cell survival and induces the senescence of untransformed cells (Gh Odke, Remisova, Furst, Kilic, & Soutoglou, 2021; Li, Liu, Meng, & Zhu, 2019). AHNAK inhibits the proliferation and metastasis of ovarian cancer and thyroid cancer cells via the Wnt/ β -catenin pathway (Bo, Jin, Dai, & Zhou..., 2017; Lin et al., 2021). AHNAK is considered as a new oncogene, whose role and mechanism in cancer need to be further explored. The expression of AHNAK has a certain effect on immune infiltration of lung adenocarcinoma cells (Zheng, Liu, Bian, Liu, & Liu, 2020). Moreover, AHNAK has a certain correlation with six kinds of immune infiltrating cells in BLCA, indicating that it is significant in tumor immunity as a new oncogene and is worthy of further exploration.

In recent years, due to the high accuracy and safety of immunotherapy, immune checkpoint inhibitors (ICIs) have been increasingly applied in clinic, which has become a prominent progress in tumor treatment (Jia et al., 2017; Spigel et al., 2018; Vari et al., 2018). The immune evasion mechanism within tumor microenvironment (TME) of advanced cancer shows high heterogeneity (Jiménez-Morales, Aranda-Uribe, Pérez-Amado, Ramírez-Bello, & Hidalgo-Miranda, 2021; Kim et al., 2021). Apart from programmed cell death protein 1 (PD-1) and its ligand (PD-L1), additional cellular or molecular mechanisms can cause immune dysfunction in TME as well (J. Liu et al., 2021; Scarpitta, Hacker, Büning, Boyer, & Adriouch, 2021). Korpál *et al.* discovered that the PPAR γ /RXR α pathway partially increased the resistance of BLCA to immunotherapy by damaging the infiltration of CD8 + T cells (Korpál et al., 2017). Although anticancer immunotherapy has provided an alternative treatment option for BLCA, there is still a small group of BLCA patients that can benefit from immunotherapy, and the recognized molecular markers for BLCA are still lacking.

Certain limitations should be noted in this study. First, the data were derived from publicly available data. Second, the number of samples decreased after excluding samples with incomplete clinical data or follow-up information. Third, computer language was used in the method. Fourth, due to the different data processing methods, there might be minor deviations from the previous research results. Last, immunotherapy is one of the most concerned areas in cancer treatment today, and there are plenty of studies on immunotherapy. So there may be duplication in the use of data, and the credibility of the results should be further verified.

In summary, the four related genes in this model include the ancient and newly discovered tumor-related genes, which mediate the pathogenesis and progression of different tumors. This study has narrowed the scope of immune genes and increased the screening criteria for the correlation between genes and diseases. In addition, TCGA-CCRCC is used as the model validation set for the sake of verifying our model feasibility and significance in urinary system tumors. It is a supplement and further verification of the previous prognostic models of BLCA, and it is also an important attempt to unify the prognostic models of urinary system tumors.

Abbreviations

A3H APOBEC3H

AUC area under the curve

BC biological processes

BLCA breast cancer

BPs Bladder cancer

CCRCC clear cell renal cell carcinoma

CCs cellular components

DCA decision curve analysis

DCs dendritic cells

DEGsDifferentially expressed genes

ESCCesophageal squamous cell carcinoma

GO Gene Oncology

ICIs immune checkpoint inhibitors

IRSS Immune Risk Scoring Characteristics

KEGG Kaplan-Meier

KM molecular functions

MFs Kyoto Encyclopedia of Genes and Genomes

OS overall survival

PD-1 programmed cell death protein 1

ROC receiver operating characteristic

TME tumor microenvironment

Declarations

Ethical Approval and Consent to participate:

Not applicable.

Consent for publication:

Not applicable.

Availability of data and material

All of the data used in this study are available online in TCGA (<https://portal.gdc.cancer.gov/>).

Competing interests:

The authors declare no conflict of interest.

Funding:

This work was supported by

1. National Natural Science Foundation of China (Grant No. 81803057)
2. Kuanren Talent Program of the Second Affiliated Hospital of Chongqing Medical University (KY2019Y2016).

Author Contributions:

Conceptualization: Jun Zheng, Weili Zhang; Methodology: Jun Zheng, Junyong Zhang; Date Analysis: Jun Zheng; Writing—Original Draft Preparation: Jun Zheng; Writing—Review and Editing: Junyong Zhang, Weili Zhang; Supervision: Junyong Zhang, Weili Zhang; Project Administration: Jun Zheng, Weili Zhang. All authors have read and agreed to the published version of the manuscript.

Acknowledgments:

Not applicable.

Authors' information:

Jun Zheng, Department of Urology, the Second Affiliated Hospital of Chongqing Medical University, 2020120934@stu.cqmu.edu.cn

Junyong Zhang, Department of Urology, the Second Affiliated Hospital of Chongqing Medical University, Zhangmachine@cqmu.edu.cn

Weili Zhang, Department of Urology, the Second Affiliated Hospital of Chongqing Medical University, 66zwl@sina.com

References

1. Alexandrov, L., Nik-Zainal, S., Wedge, D. et al. 2013. Signatures of mutational processes in human cancer. *-Nature*. 415-421
2. Bo, C., Jin, W., Dai, D. et al. 2017. AHNAK suppresses tumour proliferation and invasion by targeting multiple pathways in triple-negative breast cancer. *-Journal of Experimental & Clinical Cancer Research*. **36**
3. Candido, J., & Hagemann, T. 2013. Cancer-Related Inflammation. *-Journal of Clinical Immunology*. **33**: 79-84
4. Constantin, D., Dubuis, G., Conde-Rubio, M. d. C. et al. 2021. APOBEC3C, a nucleolar protein induced by genotoxins, is excluded from DNA damage sites. *-The FEBS Journal*.
5. Dedieu, S., & Langlois, B. 2008. LRP-1: a new modulator of cytoskeleton dynamics and adhesive complex turnover in cancer cells. *-Cell Adh Migr*. **2**: 77-80
6. DeGeorge, K. C., Holt, H. R., & Hodges, S. C. 2017. Bladder Cancer: Diagnosis and Treatment. *-American Family Physician*. **96**: 507-514
7. DeLong, E. R., DeLong, D. M., & Clarke-Pearson, D. L. 1988. Comparing the areas under two or more correlated receiver operating characteristic curves: a nonparametric approach. *-Biometrics*. **44**: 837
8. Fridman, W. H., Zitvogel, L., Sautes-Fridman, C. et al. 2017. The immune contexture in cancer prognosis and treatment. *-Nat Rev Clin Oncol*. **14**: 717-734
9. Gandellini, P., Andriani, F., Merlino, G. et al. 2015. Complexity in the tumour microenvironment: Cancer associated fibroblast gene expression patterns identify both common and unique features of tumour-stroma crosstalk across cancer types. *-Seminars in Cancer Biology*. **35**: 96-106
10. Gh Odke, I., Remisova, M., Furst, A. et al. 2021. AHNAK controls 53BP1-mediated p53 response by restraining 53BP1 oligomerization and phase separation. *-Molecular Cell*. **81**: 2596-2610.e2597
11. Grigorenko, A., Moliaka, Y., Soto, M. et al. 2004. The Caenorhabditis elegans IMPAS gene, imp-2, is essential for development and is functionally distinct from related presenilins. *-Proc Natl Acad Sci U S A*. **101**: 14955-14960
12. Gu, J., Chen, Q., Xiao, X. et al. 2016. Biochemical Characterization of APOBEC3H Variants: Implications for Their HIV-1 Restriction Activity and mC Modification. *-Journal of Molecular Biology*.
13. Hendricksen, K., & Witjes, J. A. 2007. Current strategies for first and second line intravesical therapy for nonmuscle invasive bladder cancer. *-Current Opinion in Urology*. **17**: 352-357

14. Hoos, A., Ibrahim, R., Korman, A. et al. 2010. Development of Ipilimumab: Contribution to a New Paradigm for Cancer Immunotherapy. -*Seminars in Oncology*. **37**: 533-546
15. Hornung, V., Hartmann, R., Blaser, A. A. et al. 2014. OAS proteins and cGAS: unifying concepts in sensing and responding to cytosolic nucleic acids. -*Nature Reviews Immunology*. **14**: 521-528
16. Jia, H., Truica, C. I., Wang, B. et al. 2017. Immunotherapy for Triple-Negative Breast Cancer: Existing Challenges and Exciting Prospects. -*Drug Resistance Updates*. **32**: 1-15
17. Jiménez-Morales, S., Aranda-Uribe, I., Pérez-Amado, C. et al. 2021. Mechanisms of Immunosuppressive Tumor Evasion: Focus on Acute Lymphoblastic Leukemia. -*Frontiers in Immunology*. **12**: 737340
18. Karin, M., & Clevers, H. 2016. Reparative inflammation takes charge of tissue regeneration. -*Nature*. **529**: 307-315
19. Kim, J., Seo, M., Lee, J. et al. 2021. Genomic and transcriptomic characterization of heterogeneous immune subgroups of microsatellite instability-high colorectal cancers. -*Journal for Immunotherapy of Cancer*. **9**
20. Kondratova, A. A., Cheon, H. J., Dong, B. et al. 2020. Suppressing PARylation by 2',5'-oligoadenylate synthetase 1 inhibits DNA damage-induced cell death. -*The EMBO Journal*. **39**: e101573
21. Korpál, M., Puyang, X., Jeremy Wu, Z. et al. 2017. Evasion of immunosurveillance by genomic alterations of PPAR γ /RXR α in bladder cancer. -*Nature Communications*. **8**: 103
22. Li, M., Liu, Y., Meng, Y. et al. 2019. AHNAK Nucleoprotein 2 Performs a Promoting Role in the Proliferation and Migration of Uveal Melanoma Cells. -*Cancer Biotherapy and Radiopharmaceuticals*. **34**: 626-633
23. Lillis, A. P., Duyn, L., Murphy-Ullrich, J. E. et al. 2008. LDL Receptor-Related Protein 1: Unique Tissue-Specific Functions Revealed by Selective Gene Knockout Studies. -*Physiological Reviews*. **88**: 887-918
24. Lin, Q., Qi, Q., Hou, S. et al. 2021. Silencing of AHNAK2 restricts thyroid carcinoma progression by inhibiting the Wnt/ β -catenin pathway. -*Neoplasma*.
25. Liu, J., Chen, Z., Li, Y. et al. 2021. PD-1/PD-L1 Checkpoint Inhibitors in Tumor Immunotherapy. -*Frontiers in Pharmacology*. **12**: 731798
26. Liu, Q., Luo, Y. W., Cao, R. Y. et al. 2020. Association between APOBEC3H-Mediated Demethylation and Immune Landscape in Head and Neck Squamous Carcinoma. -*BioMed Research International*. **2020**: 1-17
27. Mantovani, A., Allavena, P., Sica, A. et al. 2008. Cancer-related inflammation. -*Nature*. **454**: 436-444
28. Mathieu, R., Mathieu, R., Nadine, H. et al. 2018. Development of immunotherapy in bladder cancer: present and future on targeting PD(L)1 and CTLA-4 pathways. -*World Journal of Urology*. **36**: 1-14
29. Mbeutcha, A., Shariat, S. F., Rieken, M. et al. 2016. Prognostic significance of markers of systemic inflammatory response in patients with non muscle-invasive bladder cancer. -*Urologic Oncology-Seminars and Original Investigations*. **34**: 8

30. Noguchi, S., Yamada, N., Kumazaki, M. et al. 2013. *socs7*, a target gene of microRNA-145, regulates interferon- β induction through STAT3 nuclear translocation in bladder cancer cells. *-Cell Death & Disease*. **4**: e482
31. Padariya, M., Sznarkowska, A., Kote, S. et al. 2021. Functional Interfaces, Biological Pathways, and Regulations of Interferon-Related DNA Damage Resistance Signature (IRDS) Genes. *-Biomolecules*. **11**: 29
32. Peinemann, F., Unverzagt, S., Hadjinicolaou, A. V. et al. 2019. Immunotherapy for metastatic renal cell carcinoma: A systematic review. *-Journal of Evidence-Based Medicine*. **12**: 253-262
33. Rey-Cárdenas, M., Guerrero-Ramos, F., Lista, A. G. d. L. et al. 2021. Recent advances in neoadjuvant immunotherapy for urothelial bladder cancer: What to expect in the near future. *-Cancer Treatment Reviews*. **93**: 102142
34. Sakamoto, H., Koma, Y. I., Higashino, N. et al. 2021. PAI-1 derived from cancer-associated fibroblasts in esophageal squamous cell carcinoma promotes the invasion of cancer cells and the migration of macrophages. *-Laboratory investigation; a journal of technical methods and pathology*. **101**: 353-368
35. Sanjeev Sharma, P. K., Poonam Sharma. 2009. Diagnosis and treatment of bladder cancer. *-American Family Physician*. **80**: 717-723
36. Scarpitta, A., Hacker, U., Büning, H. et al. 2021. Pyroptotic and Necroptotic Cell Death in the Tumor Microenvironment and Their Potential to Stimulate Anti-Tumor Immune Responses. *-Frontiers in oncology*. **11**: 731598
37. Shi, M. J., Meng, X. Y., Lamy, P. et al. 2019. APOBEC-mediated Mutagenesis as a Likely Cause of FGFR3 S249C Mutation Over-representation in Bladder Cancer. *-European Urology*.
38. Siegel, R. L., Miller, K. D., & Jemal, A. 2015. Cancer statistics, 2015. *-CA: A Cancer Journal for Clinicians*. **65**
39. Spigel, D. R., Reynolds, C., Waterhouse, D. et al. 2018. Phase 1/2 Study of the Safety and Tolerability of Nivolumab Plus Crizotinib for the First-line Treatment of ALK Translocation-Positive Advanced Non-Small Cell Lung Cancer (CheckMate 370). *-Journal of Thoracic Oncology*. **13**: S155608641830176X
40. Theret, L., Jeanne, A., Langlois, B. et al. 2017. Identification of LRP-1 as an endocytosis and recycling receptor for B1-integrin in thyroid cancer cells. *-Oncotarget*. **8**: 78614-78632
41. Thomas, Powles, Joseph et al. 2014. MPDL3280A (anti-PD-L1) treatment leads to clinical activity in metastatic bladder cancer. *-Nature*. **515**: 558-562
42. Vari, F., Arpon, D., Keane, C. et al. 2018. Immune evasion via PD-1/PD-L1 on NK-cells and monocyte/macrophages is more prominent in Hodgkin lymphoma than DLBCL. *-Blood*. **131**: 1809-1819
43. Wallach, David, Kang et al. 2014. Concepts of tissue injury and cell death in inflammation: a historical perspective. *-Nature Reviews Immunology*.
44. Yang, R., Chang, Q., Meng, X. et al. 2018. Prognostic value of Systemic immune-inflammation index in cancer: A meta-analysis. *-Journal of Cancer*. **9**: 3295-3302

45. Yu, S. S., Ballas, L. K., Skinner, E. C. et al. 2017. Immunotherapy in urothelial cancer, part 2: adjuvant, neoadjuvant, and adjunctive treatment. -*Clin Adv Hematol Oncol.* **15**: 543-551
46. Zeng, J. H., Liang, L., He, R. Q. et al. 2017. Comprehensive investigation of a novel differentially expressed lncRNA expression profile signature to assess the survival of patients with colorectal adenocarcinoma. -*Oncotarget.* **8**
47. Zhang, Y., & Yu, C. 2020. Prognostic characterization of OAS1/OAS2/OAS3/OASL in breast cancer. -*BMC Cancer.* **20**: 575
48. Zheng, M., Liu, J., Bian, T. et al. 2020. Correlation between prognostic indicator AHNAK2 and immune infiltrates in lung adenocarcinoma. -*International Immunopharmacology.* **90**: 107134

Figures

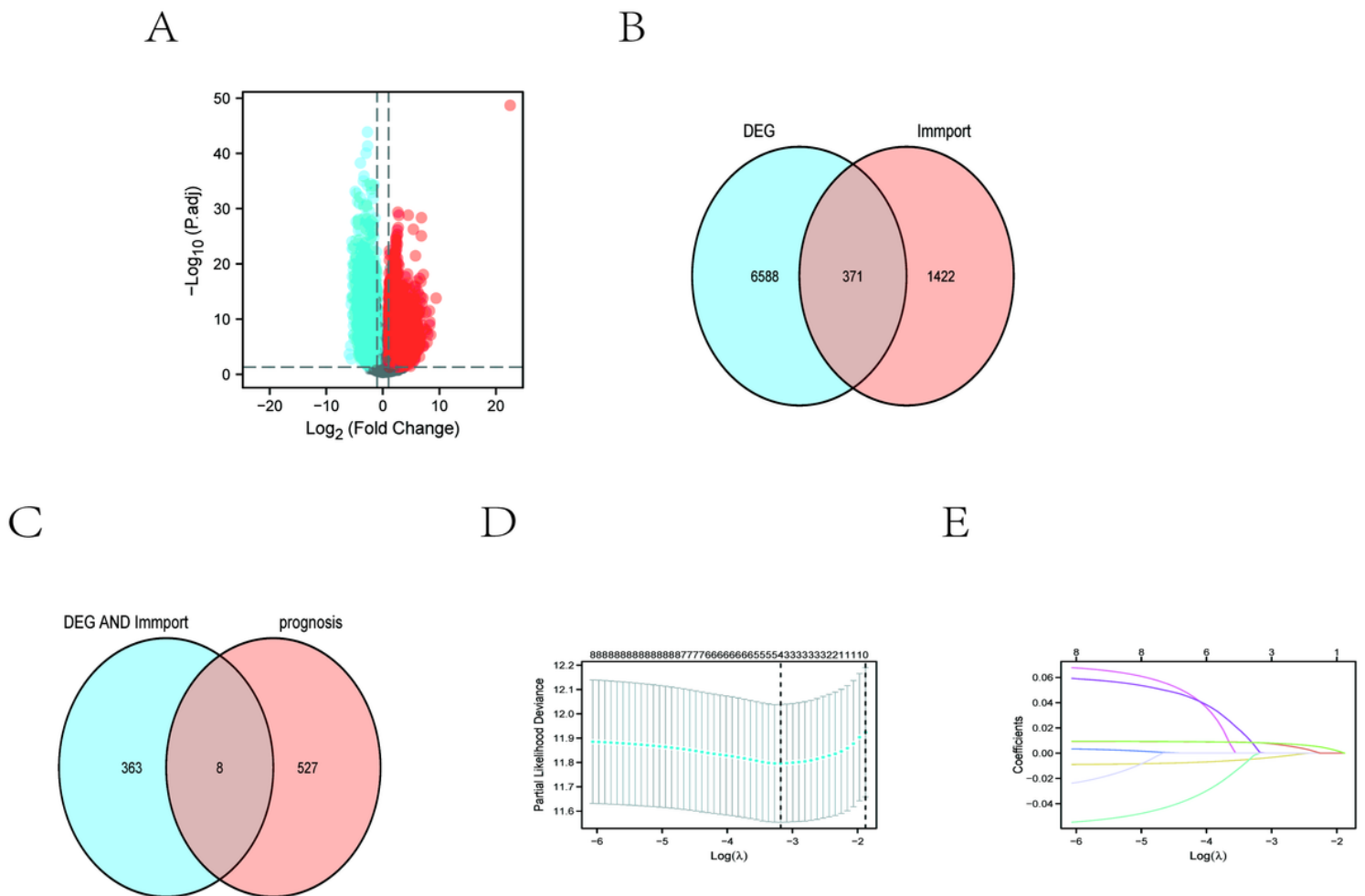


Figure 1

Screening of IRSS Signature. (A) Volcano plot of 1479 differentially expressed genes. (B) Venn diagram of the intersection of DEGs and immune genes. (C) Venn diagram of the intersection of DEGs, immune

genes and prognostic genes. (D) Ten-time cross-validation for tuning parameter selection in the LASSO model. (E) LASSO coefficient profiles.

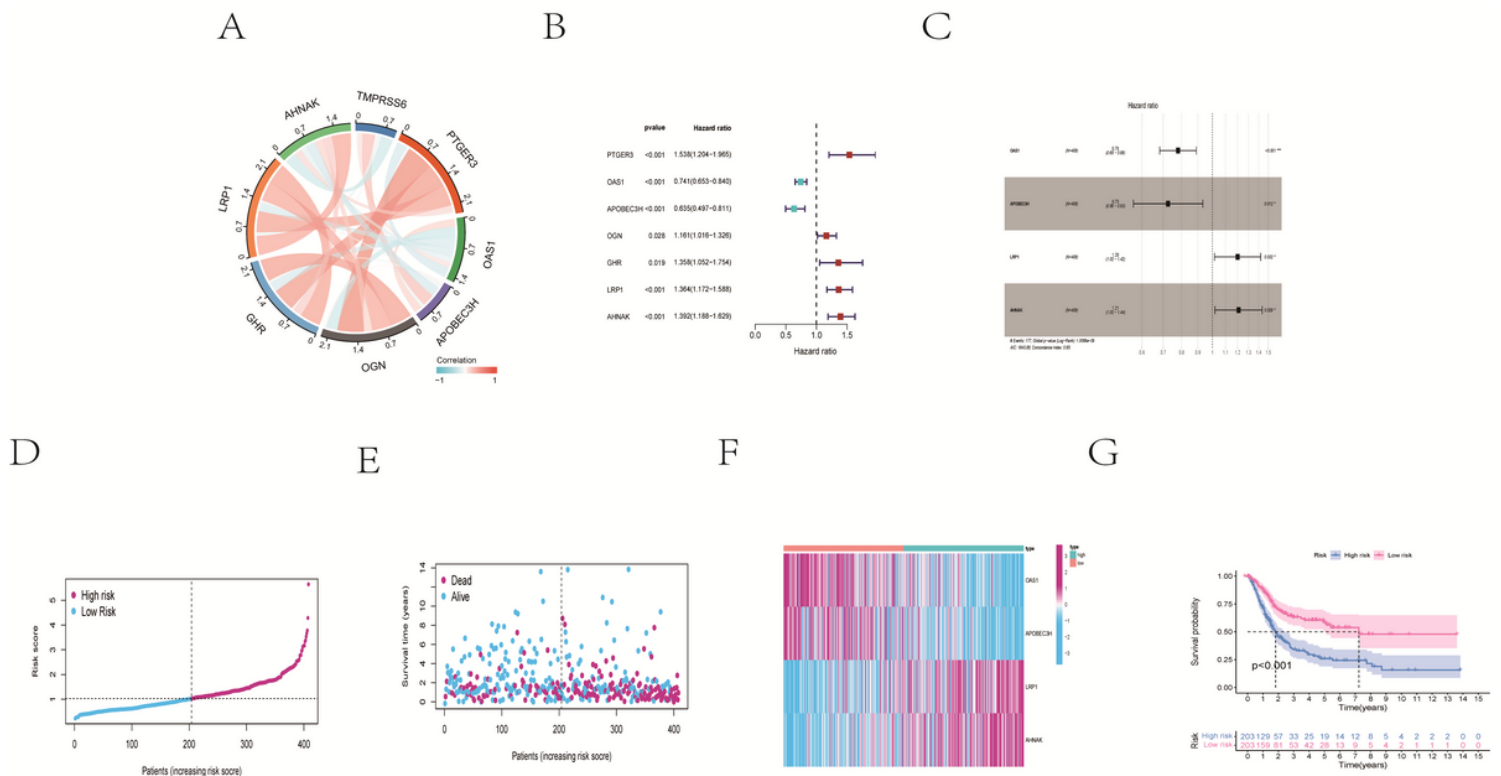


Figure 2

Establishment of IRSS Signature. (A) correlation of eight immune-related differential genes. The hazard ratios of genes integrated into the IRSS signatures are shown in the forest plots for BLCA based on Univariate Cox regression analyses(B) and multivariate Cox regression analyses(C). Distribution of risk scores(D), along with survival statuses(E), and gene expression profiles(F) for BLCA. (G)Kaplan-Meier curves show that OS was significantly different between the high- and low-risk groups in TCGA-BLCA.

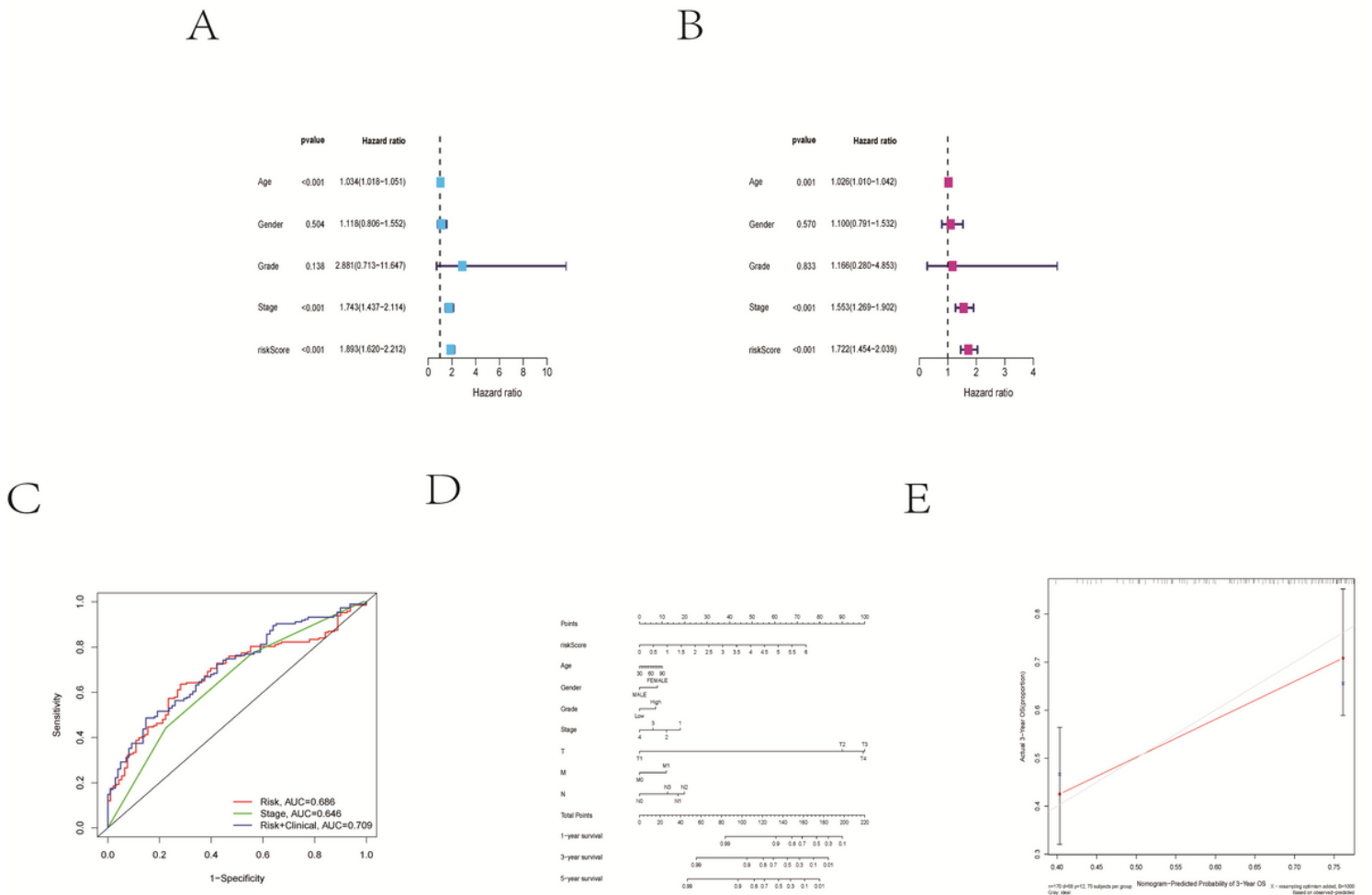
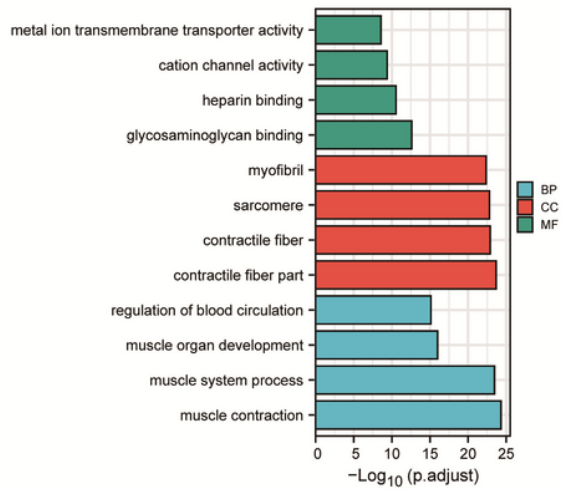


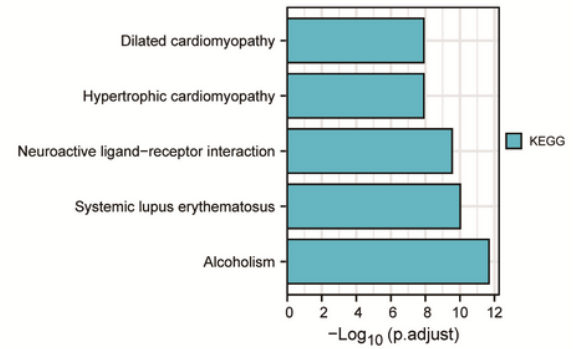
Figure 3

Evaluation of IRSS signatures and establishment and evaluation of nomograms. Univariate (A) and multivariate (B) independent prognostic analysis of independent risk factors for OS in patients with BLCA. (C) Time-independent ROC analysis of risk scores for OS prediction in the TCGA database. (D) A nomogram for predicting 1-, 3- and 5-year survival possibilities of individual BLCA patients. The calibration curve of 3-year (E) survival of BLCA patients. The 45° grey line represented a perfect uniformity between nomogram-predicted and real possibilities.

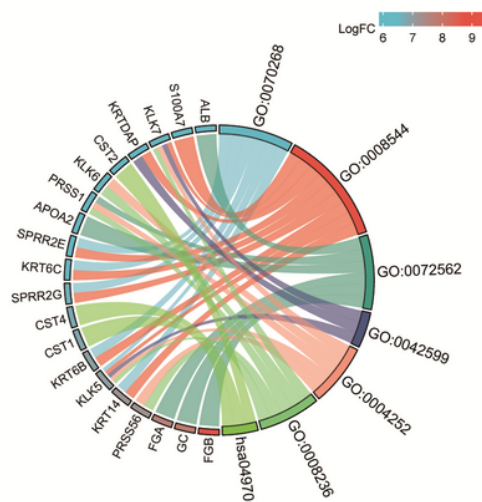
A



B



C



D

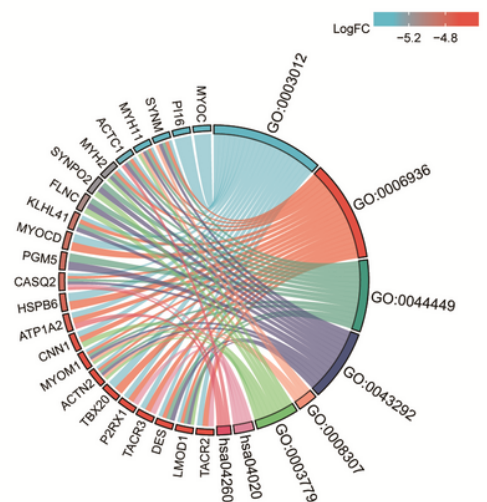


Figure 4

Gene functional enrichment analysis. (A) GO-term function enrichment analysis of all differentially expressed genes. (B) KEGG-term function enrichment analysis of all differentially expressed genes. GO and KEGG function enrichment analysis of the up-regulated (C) and down-regulated DEGs (D) in BLCA cohort were displayed by the chord diagrams

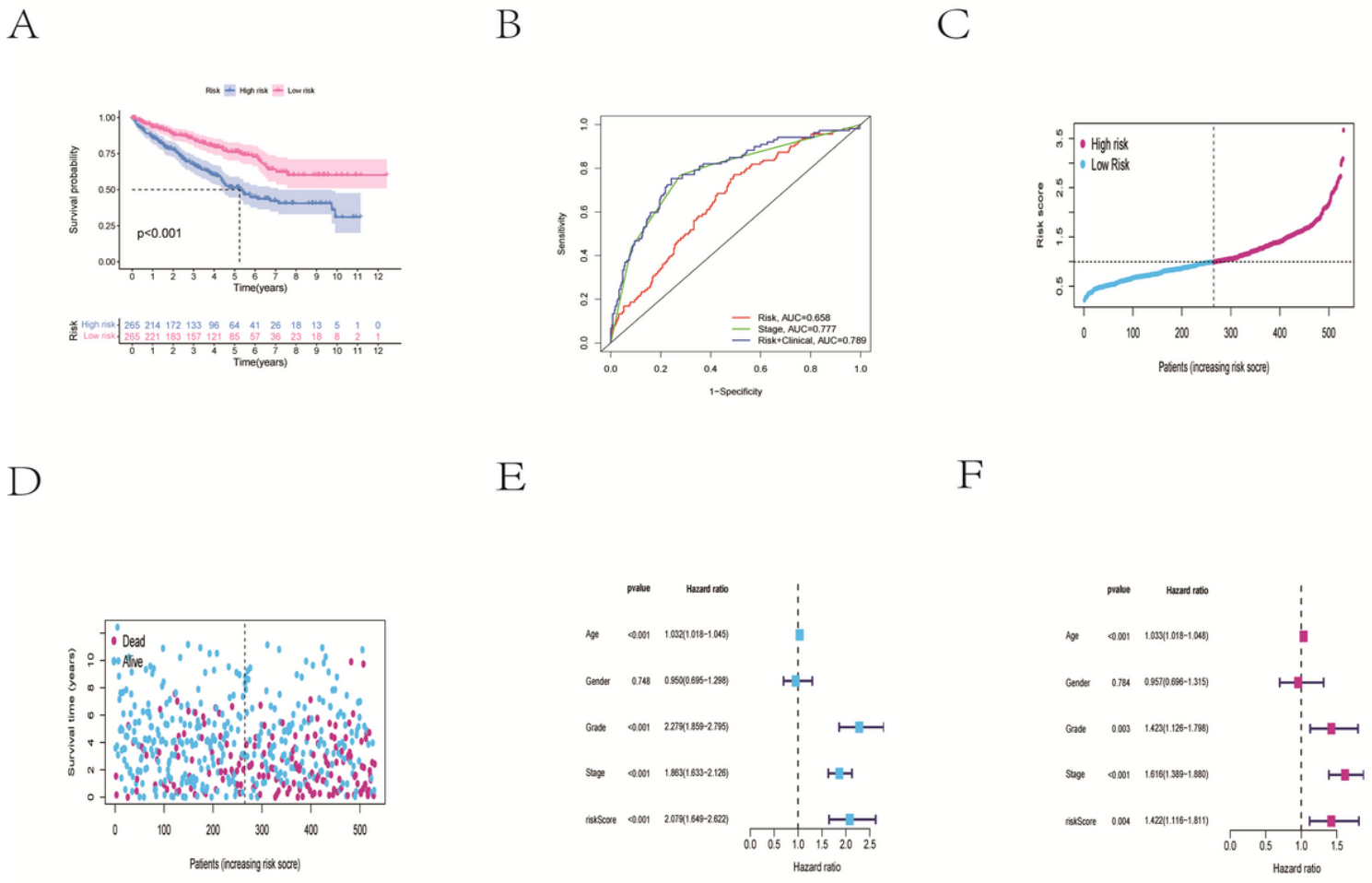


Figure 5

Validation of IRSS signature with TCGA-CCRCC. (A) Kaplan-Meier curves show that OS in the low-risk was significantly higher than in the high-risk group. (B) Time-dependent ROC curve analysis of the IRSS at 3 years. Distribution of risk scores(C), along with survival statuses(D), Univariate (E) and multivariate (F) independent prognostic analysis of independent risk factors for OS in patients with CCRCC.

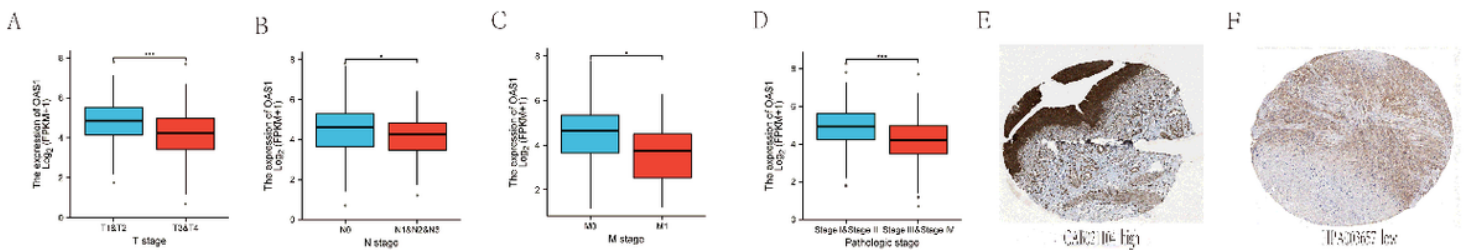


Figure 6

Relationships between OAS1 mRNA levels and clinical pathological characteristics and immunohistochemistry of OAS1 protein in urinary bladder tissue and urothelial cancer patients from the the human protein atlas database. OAS1 mRNA expression was significantly correlated with T stage(A), N

stage(B), M stage(C), pathologic stage (D).(ns, no significance, *P < 0.05, **P < 0.01, ***P < 0.001). (E)The urothelial cells staining was high. (F)The tumor cells staining was low.

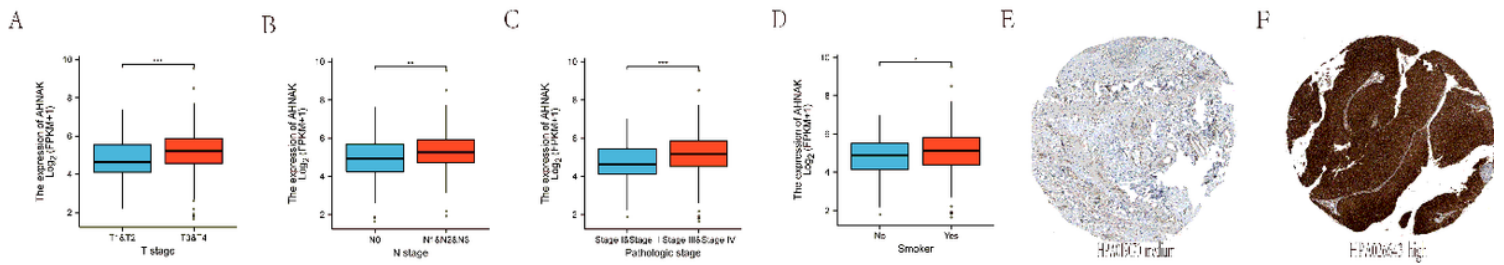


Figure 7

Relationships between AHNAK mRNA levels and clinical pathological characteristics and Immunohistochemistry of AHNAK protein in urinary bladder tissue and urothelial cancer patients from the the human protein atlas database. AHNAK mRNA expression was significantly correlated with T stage(A), N stage(B),pathologic stage (C) and smoker(D).(ns, no significance, *P < 0.05, **P < 0.01, ***P < 0.001). (E)The urothelial cells staining was medium. (F)The tumor cells staining was high.

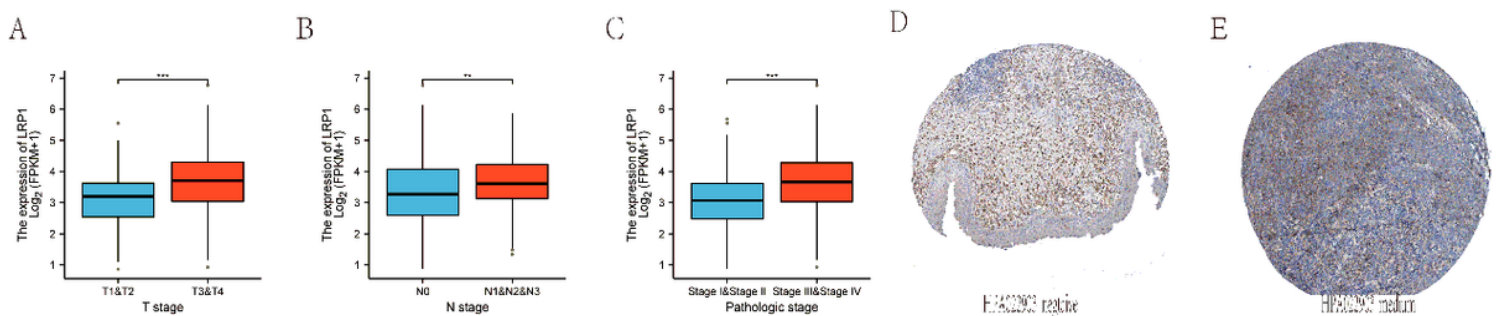


Figure 8

Relationships between LRP1 mRNA levels and clinical pathological characteristics and Immunohistochemistry of LRP1 protein in urinary bladder tissue and urothelial cancer patients from the the human protein atlas database. LRP1 mRNA expression was significantly correlated with T stage(A), N stage(B) and pathologic stage (C).(ns, no significance, *P < 0.05, **P < 0.01, ***P < 0.001). (D)The urothelial cells staining was negative. (F)The tumor cells staining was medium.

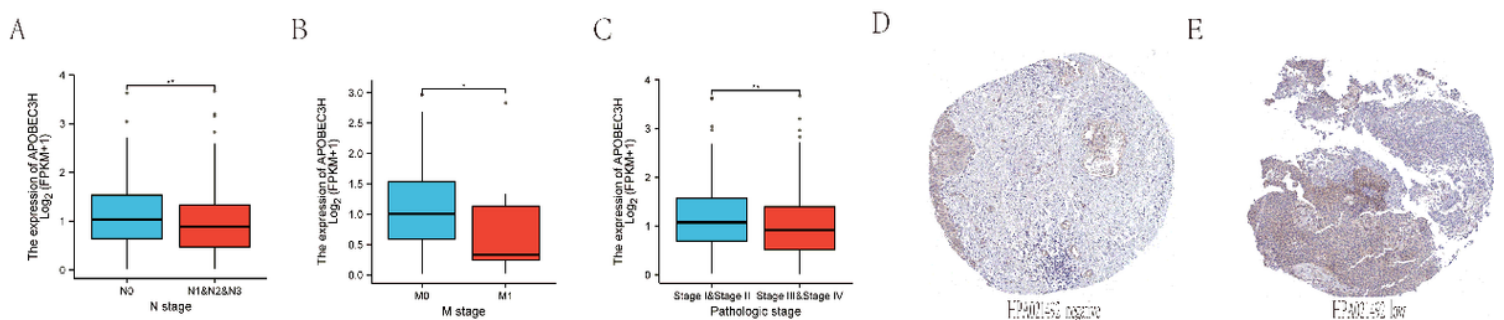
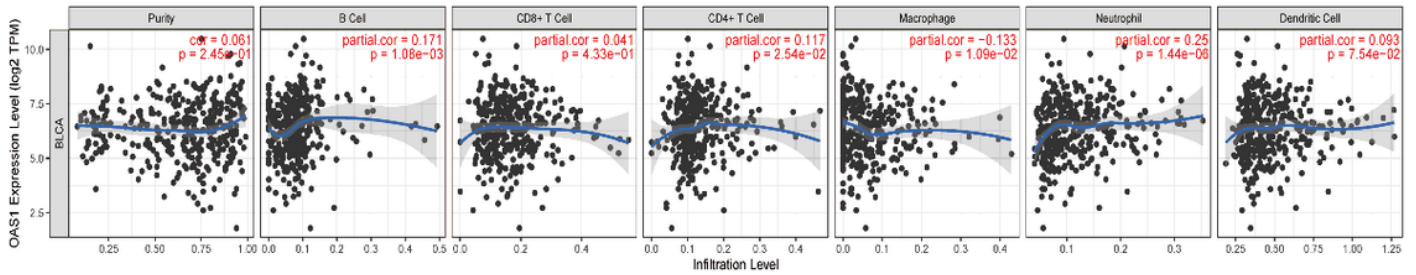


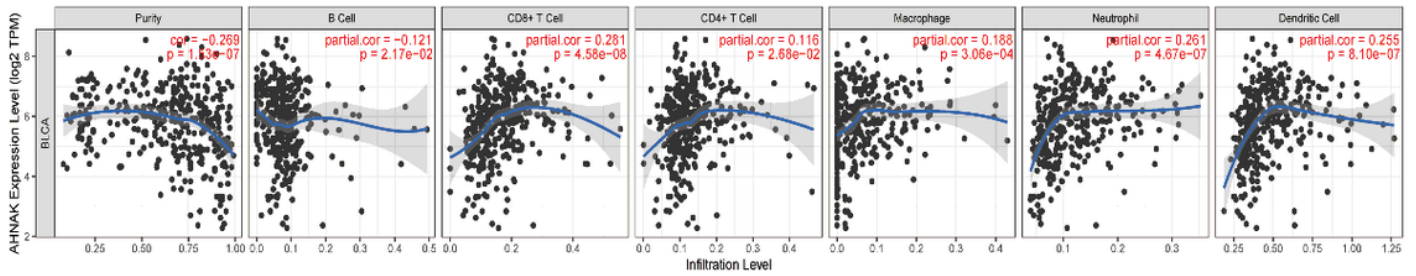
Figure 9

Relationships between APOBEC3H mRNA levels and clinical pathological characteristics and Immunohistochemistry of APOBEC3H protein in urinary bladder tissue and urothelial cancer patients from the the human protein atlas database. APOBEC3H mRNA expression was significantly correlated with N stage(A), M stage(B) and pathologic stage (C).(ns, no significance, *P < 0.05, **P < 0.01, ***P < 0.001). (D)The urothelial cells staining was negative. (F)The tumor cells staining was low.

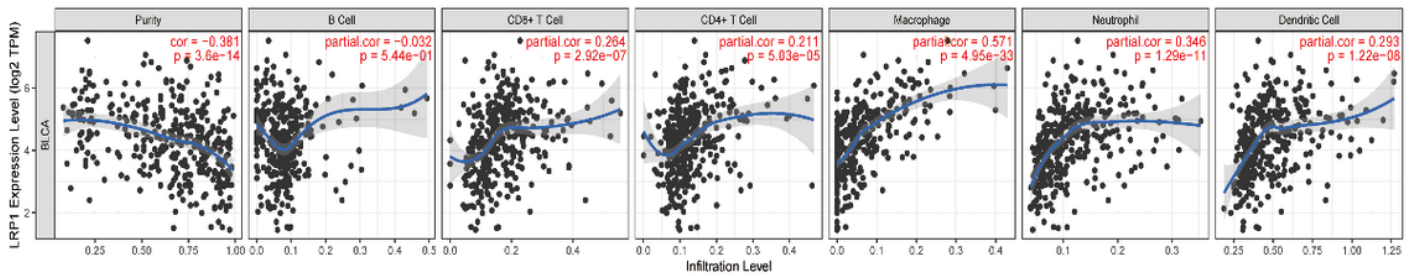
A



B



C



D

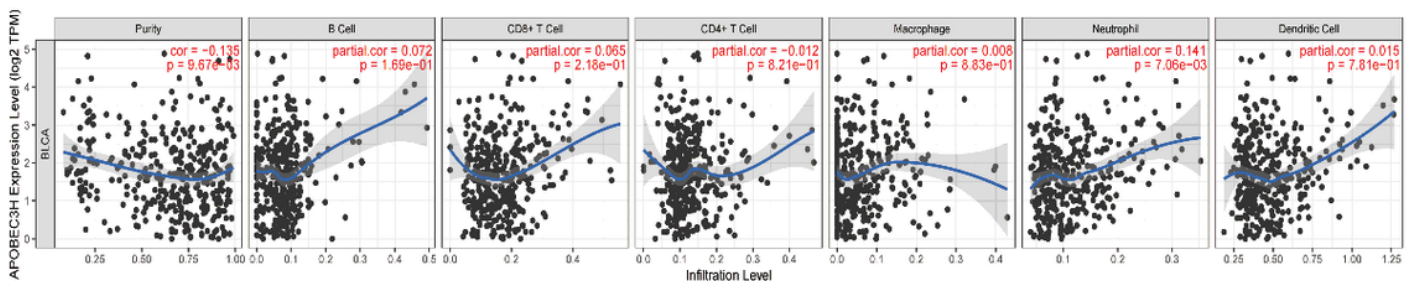


Figure 10

The relationship between model genes and immune cell infiltration in BLCA. The OAS1, AHNAK, LRP1 and APOBEC3H expression results of six tumor-infiltrating immune cells in BLCA from The Tumor database.

Supplementary Files

This is a list of supplementary files associated with this preprint. Click to download.

- [OAS1.png](#)